

Effect of Axial Ligand Plane Reorientation on Electronic and Electrochemical Properties Observed in the A67V Mutant of Rat Cytochrome b_5

Siddhartha Sarma,[‡] Russell J. DiGate,[‡] David B. Goodin,[§] Cary J. Miller,^{*,||} and R. D. Guiles^{*,‡}

Department of Pharmaceutical Sciences, School of Pharmacy, University of Maryland at Baltimore, and Medical Biotechnology Center, Maryland Biotechnology Institute, University of Maryland, Baltimore, Maryland 21201, Department of Chemistry and Biochemistry, University of Maryland, College Park, Maryland 20742, and Department of Molecular Biology, MB8, The Scripps Research Institute, 10666 Torrey Pines Road, La Jolla, California 92037

Received July 26, 1996; Revised Manuscript Received February 25, 1997[⊗]

ABSTRACT: Mutational studies directed at evaluating the effect of the axial ligand plane orientation on electrochemical properties of cytochrome b_5 have been performed. As described in the previous paper, structural consequences of one of these mutations, the A67V mutation, have been evaluated using NMR solution methods. The lack of large shifts relative to the wild-type protein in both the imidazole N δ nitrogen and proton resonances of the H63 imidazole ring indicates that the hydrogen bond between the carbonyl of F58 and the imidazole ring of H63 remains intact in this mutant. Effects of the imidazole plane reorientation on the Fe d-orbitals were evaluated on the basis of interpretation of EPR spectra, near-infrared bands associated with ligand-to-metal charge transfer transitions, reorientation of the anisotropy of the paramagnetic center determined by calculation of pseudocontact shifts, and the temperature dependence of the contact-shifted resonances. The dominant effect of the imidazole reorientation appears to have been a destabilization of the d_{xz} orbital energy and a reorientation of the d_{xy} orbitals. This is surprising in light of the -20 mV shift in the reduction potential of the mutant relative to the wild-type protein and indicates that a destabilization of d_{yz} -orbital energy level of the reduced state dictates the observed change in reduction potential. Measured values for the reorganizational energy and heterogeneous electron transfer rates were indistinguishable for wild-type and mutant proteins. This is perhaps surprising, given significant differences in the pattern of electron delocalization into the porphyrin ring observed as significantly altered contact shift patterns. Mutational studies perturbing the H39 imidazole were also performed but with more limited success.

Cytochrome b_5 is one of the most extensively studied of the b-type cytochromes [for a review see Mathews (1985)]. It has become a model system for understanding structure–function relationships modulating electrochemical properties of b-type cytochromes (Reid et al., 1987; Walker et al., 1988; Dixon et al., 1990). In addition to extensive studies of the wild-type protein, including many species variants, site-directed mutagenesis has become an important tool for understanding elements of protein structure important in determining electrochemical properties of cytochromes (Funk et al., 1990; Rodgers & Sliagar, 1991).

Current theories regarding the mechanisms proteins use to control reduction potentials of the heme cofactor fall into three categories: (1) the protein environment provides a variable dielectric matrix which modulates stability of the iron center (Langen et al., 1992; Zhou, 1994); (2) hydrogen bonding to the axial imidazole ligands has been hypothesized to be an important reduction potential regulation factor (Quin et al., 1984; Goodin & McRee, 1993); and (3) orientation of the axial imidazole ligand planes has been proposed to play a significant role in modulating Fe d_{xy} energy levels through bonding interactions and/or electrostatic repulsion

(Safo et al., 1991). It is this latter class of effects which is the focus of this work.

Other electrochemical properties of hemes which have been proposed to be modulated by the protein matrix include the following: (1) outer sphere reorganizational energy, modulated by the low dielectric of the protein matrix, has been proposed to facilitate long-range interprotein biological electron transfer by reducing outer sphere reorganizational energy in protein complexes (Zhou, 1994); (2) a growing body of evidence now clearly implicates details of the protein structure important in the electronic coupling between redox centers in long-range biological electron transfer (Siddarth & Marcus, 1993). Theoretical studies of electronic coupling employ relatively severe approximations with regard to the number and parametrization of orbitals involved in coupling redox-active centers within a protein complex (Friesner, 1994). Thus, experimental measures of electronic coupling and reorganization energy under varying protein conditions could provide significant additional data necessary to accurate parametrization of semiempirical formalisms.

In this report we examine the results of novel experimental approaches to the study of reorganizational energy and electronic coupling in cytochromes using surface-modified electrodes (Becka & Miller, 1992; Terretaz et al., 1996) and evaluate the results obtained in terms of knowledge of the electronic and physical properties of the proteins gained through a number of spectroscopic probes of the system. Electronic coupling is measured to the electrode, presumably

* To whom correspondence should be addressed.

[‡] Department of Pharmaceutical Sciences and Maryland Biotechnology Institute, University of Maryland.

[§] Department of Chemistry and Biochemistry, University of Maryland.

^{||} The Scripps Research Institute.

[⊗] Abstract published in *Advance ACS Abstracts*, April 15, 1997.

mediated through the exposed heme edge in cytochrome *b*₅ and site-directed mutants of the protein. It is suggested that this model is a realistic mimic of interactions of cytochrome *b*₅ with electron transfer partners which have been examined, either experimentally, theoretically, or both [e.g., such as cytochrome *c* (Salemme, 1976; Wendoloski et al., 1985), myoglobin (Livingston et al., 1985), hemoglobin (Poulos & Mauk, 1983), and cytochrome P450 (Stayton et al., 1989)]. The lack of significant differences in electronic coupling observed between wild-type cytochrome *b*₅ and a site-directed mutant of cytochrome *b*₅ is discussed in light of differences in contact coupling between the largely non-bonding d-orbitals of the iron and the porphyrin π -orbitals observed as differences in the pattern of contact shifted resonances. Delocalization of unpaired spin density into the heme molecular orbital system is qualitatively interpreted in an analysis of shifts in contact shift patterns. It is important to point out that the contact coupling between the unpaired spin of the iron center and the porphyrin π -system and the electronic coupling between the electrode and the redox active center are different physical phenomena. However, we believe that the pattern of delocalization of unpaired spin density into the porphyrin π -system must be related to the dominant electronic coupling path in this system in that the orbital containing the unpaired spin is also the orbital into which the reducing equivalent must be placed, and the heme edge itself is the point of closest approach of the redox-active center to the electrode.

MATERIALS AND METHODS

Electrochemistry. All electrochemical experiments were performed using a jacketed conical cell which allowed measurements to be made at controlled temperatures using volumes as small as 150 μ L. A BAS-100A electrochemical analyzer was used for all measurements. All solutions were purged with N₂ before use and blanketed with N₂ during the electrochemical determinations. Au electrodes were prepared by sputtering a *ca.* 500 Å Cr adhesion layer followed by a *ca.* 3000 Å Au layer through a special mask defining the electrode pattern. The electrodes were 0.13 cm² in area. Immediately prior to the derivatization with thiols, the electrodes were cleaned through successive 30 s exposures to 1% K₂Cr₂O₇ in concentrated H₂SO₄ at 60 °C and 3% aqueous HF at 25 °C. Each of these exposures was followed by extensive rinsing with deionized water. The electrodes were derivatized with self-assembled monolayers of ω -hydroxyalkanethiols by 30 min to 16 h exposures to a *ca.* 20 mM solution of the thiol in 95% ethanol.

The formal potentials of the cytochromes were determined using Au electrodes coated with short chain length ω -hydroxyalkanethiol monolayers [HO(CH₂)₃SH or HO(CH₂)₄SH]. The average of the cathodic and anodic peak potentials was taken as the formal potential. All potentials were measured versus a saturated calomel reference (SCE)¹ and are reported versus the standard hydrogen potential (NHE). All electrochemical measurements were performed on 2–4 mM solutions of the cytochromes in 0.1–1.0 M KCl, 1 mM

phosphate buffer, pH 7.0 at 25 °C. The uncertainties in the measurement of the reduction potentials are estimated from repeated measurements to be ± 3 mV.

Electrochemical Data Analysis. Kinetic parameters for the reduction of the cytochromes were extracted from voltammograms obtained using Au electrodes coated with HO(CH₂)₁₁SH monolayers. The current/voltage curves were corrected for both diffusion and double layer effects as described previously (Terretaz et al., 1995). These corrected current/voltage curves were normalized to unit electrode area (1 cm²) and unit concentration of the redox molecule (1/F mol/cm³ or 10.36 mM) to yield the heterogeneous electron transfer rate constant as a function of the applied formal overpotential ($E_{\text{applied}} - E_0'$). The reorganization energy for the cytochromes was determined as the peak in a plot of the derivative of the heterogeneous electron transfer rate. The maximum heterogeneous electron transfer rate, k_{max} , was determined by integrating the best fit Gaussian curve through the derivative plot. Estimates of the solvent-accessible surface areas of the exposed hemes based on the crystal structures of horse cytochrome *c* (Bushnell et al., 1990) and bovine cytochrome *b*₅ (Mathews et al., 1979) were performed using the program ms, which is part of the Midas II Plus distribution package (Langridge et al., 1981).

Electron Paramagnetic Resonance Spectra. EPR spectra were collected for samples containing 50% glycerol and 100 mM phosphate buffer (pH 7.0). Spectra were collected at 9.51 GHz on a Bruker ESP 300 spectrometer at 12 K using an Air Products LTR3 liquid helium cryostat as previously described (Goodin & McRee, 1993). Instrument settings are indicated in the figure legend.

Near-Infrared Spectra. Near-IR spectra were recorded using a Varian Carey 2300 UV–visible NIR spectrometer. Solutions containing 2 mM cytochrome *b*₅ proteins in 100 mM phosphate buffer (pD 7.0) lyophilized and resolubilized in 99.997% D₂O (Cambridge Isotopes) were used in recording near-IR spectra. Difference spectra were recorded relative to reference samples prepared under identical conditions but reduced with small quantities of solid sodium dithionite. As a control, NIR spectra of horse heart cytochrome *c* were recorded which reproduced literature peak maxima (Schejter & Eaton, 1984).

NMR Spectra. One-dimensional wide-spectral-width NMR spectra of the oxidized proteins were recorded at 600 MHz on a Bruker DMX Avance 600 NMR spectrometer with a spectral width of 40 000 Hz. Spectra of the oxidized proteins were recorded using 3 mM solutions of wild type and the A67V mutation in 100 mM phosphate buffer (pD 7.0) exchanged into D₂O by repeated lyophilization and resolubilization of samples. Two-dimensional NOESY spectra with short relaxation delays (50 ms) and 50 ms mixing times were recorded at 500 MHz on a Bruker AMX NMR spectrometer as described by LaMar and deRopp (1993). All proton NMR frequencies are reported relative to an internal TSP reference. Two-dimensional ¹H–¹⁵N NOESY-relayed HSQC spectra were recorded on reduced wild-type and mutant proteins at 600 MHz on a Bruker DMX Avance spectrometer. Spectra were recorded with proton and nitrogen spectral widths of 9600 and 4800 Hz, respectively, with a NOE mixing time of 100 ms. All NMR spectra were processed on a Silicon Graphics workstation using Felix 2.3 or 95.0 software (Biosym Technologies Inc.). Analysis of the temperature dependence of the contact shifted resonances

¹ Abbreviations: EPR, electron paramagnetic resonance; NMR, nuclear magnetic resonance; NIR, near-infrared spectroscopy; NHE, normal hydrogen electrode; SCE, saturated calomel electrode; NOESY, nuclear Overhauser effect spectroscopy; HSQC, heteronuclear single quantum coherence; TSP, tetra deuterio trimethylsilyl propionate.

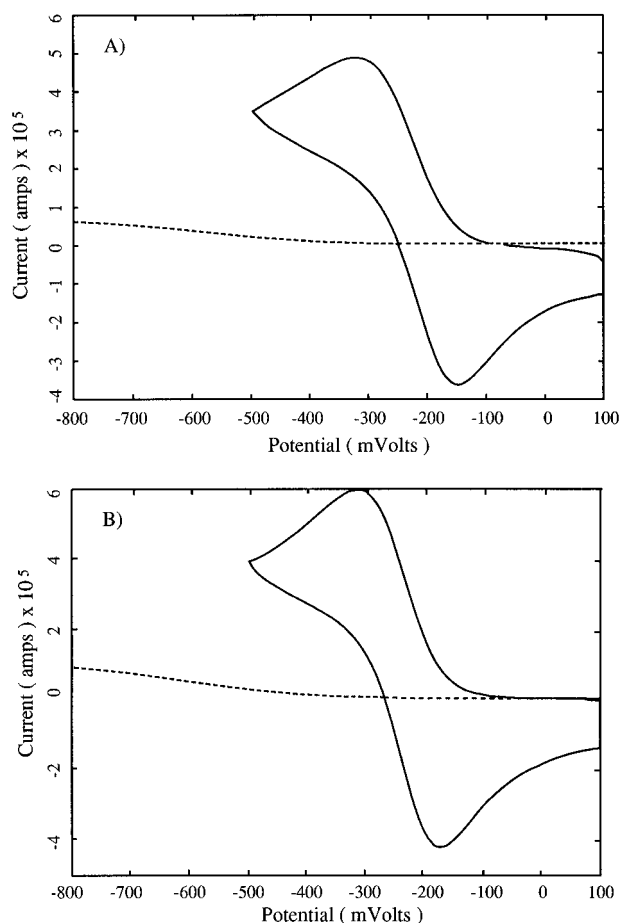


FIGURE 1: Overlay of voltammograms for (A) wild-type cytochrome b_5 and (B) the A67V mutation. Voltammograms were recorded using surface-modified electrodes with adsorbed ω -hydroxyalkanethiols containing 3-methylene units (solid curves) and 11-methylene units (dashed traces). The voltammograms employing the ω -hydroxyalkanethiols containing 3-methylene units were used to determine the reduction potentials while the voltammograms employing the ω -hydroxyalkanethiols containing 11-methylene carbons were used to determine reorganizational energies and heterogeneous electron transfer rates.

was performed on a Silicon Graphics workstation using a set of FORTRAN programs which employed minimization algorithms supplied by Numerical Recipes (Press et al., 1992).

Expression, Mutagenesis, Purification, and Labeling. Procedures describing plasmid construction and site-directed mutagenesis are described in detail in the accompanying paper (Sarma et al., 1997). Procedures for purification and labeling of wild-type and mutant cytochromes b_5 which were modifications of procedures described by von Bodman et al. (1986) are also described in the accompanying paper.

RESULTS

Electrochemical Analyses. The direct determination of the redox properties of redox proteins is often rendered impossible due to the strong adsorption of the protein onto the electrode surface. This protein adsorption passivates the electrode. The use of ω -hydroxyalkanethiol-coated Au electrodes virtually eliminates this problem. In addition, the ability to control the length of the thiol monolayer allows one to control the absolute heterogeneous electron transfer rate of the solution cytochrome. As seen in Figure 1, Au electrodes derivatized with relatively short ω -hydroxyal-

kanethiol monolayers [such as $\text{HO}(\text{CH}_2)_4\text{SH}$] give quasi-reversible voltammetric responses for both the wild-type and A67V mutant cytochrome b_5 solutions. In contrast, the dotted voltammograms obtained using the Au electrodes coated with the longer monolayer [$\text{HO}(\text{CH}_2)_{11}\text{SH}$] are significantly attenuated from the diffusion-controlled response.

From the voltammograms obtained using the Au electrodes derivatized by the shorter ω -hydroxyalkanethiol monolayers, a shift of -20 mV from the wild-type reduction potential was observed for the A67V mutation. This shift was in a direction opposite to that expected given the design philosophy of the mutation and the nature of the reorientation of the axial imidazole described in the accompanying paper (Sarma et al., 1997). However, as will be seen, the origin of the shift is not as straightforward as originally anticipated. An even larger shift of more than -100 mV was estimated for the G42A, L46N double mutant. Unfortunately, due to instability of this mutant protein only an irreversible, cathodic wave could be observed.

In addition to limiting passivation of the electrode via protein adsorption, these ω -hydroxyalkanethiol monolayers allow one to characterize the redox reactivity of the cytochromes with remarkable specificity and precision. By choosing a sufficiently thick insulating monolayer, one can slow the absolute heterogeneous electron transfer rate between the electrode and solution cytochrome to an extent at which diffusion limitations are minimized. For small redox molecules such as ferricyanide or ruthenium hexamine, a $\text{HO}(\text{CH}_2)_{14}\text{SH}$ monolayer is required to slow the electron transfer rate so that kinetic measurements can be made over the entire voltammetric limit of the coated electrode (ca. 1.0 to -0.75 V vs NHE). Interestingly, due to the shielded nature of the cytochrome b_5 , a shorter thiol monolayer [$\text{HO}(\text{CH}_2)_{11}\text{SH}$] should be used to give the same result.

A special strength of this insulated electrode voltammetric technique is that the redox properties of a molecule can be probed over a wide range of electrode potentials. Analysis of the kinetic data yields a direct measurement of the redox molecule's reorganization energy and relative electronic coupling. The derivative of the heterogeneous electron transfer rate constant as a function of the overpotential gives a measure of the density of electronic states function for the solution redox molecule. Figure 2 shows representative derivative plots for the wild-type and A67V cytochromes b_5 . The Marcus theory of electron transfer predicts that this density of electronic states distribution should be Gaussian in shape. The solid curve through the data points corresponds to the best fit Gaussian curve through the data.

The peak of the density of electron states distribution occurs at the reorganization voltage. At this potential, the cytochrome can be reduced without activation. Electrons at the Fermi level in the electrode achieve a maximal transfer rate at this reorganization voltage. At more negative potentials, the rate of electron transfer for electrons at the Fermi level decreases consistent for an electron transfer reaction in the Marcus inverted region. The reorganization energy of the cytochrome is simply obtained from the position of this peak. The reorganization energies of the wild-type and A67V mutant cytochromes b_5 are identical within experimental error as seen in Table 1. At 0.5 eV, this measured reorganization energy is over a factor of 2

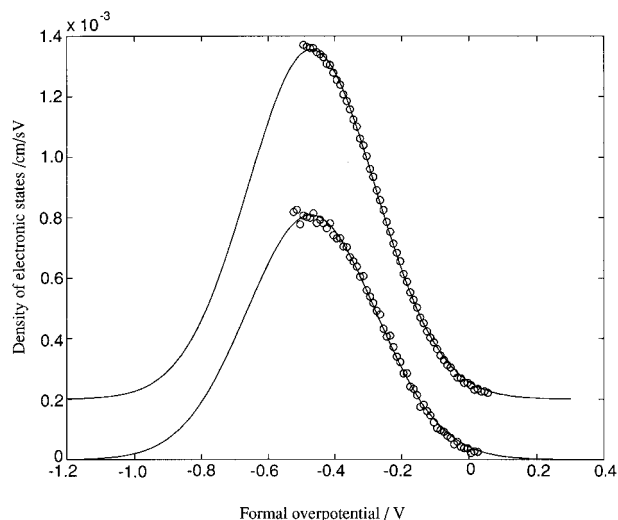


FIGURE 2: Derivative voltammograms for the A67V mutant (offset 0.2 unit of the vertical scale) and the wild-type cytochrome b_5 . Also shown as solid curves are the best Gaussian fits to the data (shown as open circles). Voltammograms were recorded using surface-modified electrodes with adsorbed ω -hydroxyalkanethiols containing 11-methylene units.

Table 1: Electrochemical Properties of Wild-Type Rat Cytochrome b_5 and Site-Directed Mutants^a

protein	E_0^b (mV)	λ (eV)	k_{\max}^c (cm/s)
wild type	16.2 ± 3	0.53 ± 0.06	$5 \times 10^{-4} \pm 1 \times 10^{-4}$
A67V	-2.8 ± 3	0.51 ± 0.06	$4 \times 10^{-4} \pm 1 \times 10^{-4}$
L46N,G42A ^d	-132.0	~ 0.5	

^a Measurements were performed at 0 °C and pH 7.0, 0.88 M KCl, 1.0 mM phosphate buffer, using a scan rate of 500 mV/s. Electrode capacitance = $2.1 \mu\text{F}/\text{cm}^2$. ^b E_0 values are reported relative to NHE. ^c Calculation of rates was performed assuming an effective local charge of -2 . ^d Electrochemical parameters for the double mutant are estimates based on an irreversible cathodic wave.

lower than that determined by Dixon et al. (1990). In this previous work, the reorganization energy was calculated from a single self-exchange rate. In order for such a single rate calculation of the reorganization energy to be accurate, one must correctly assign the preexponential term in the rate equation. Unfortunately, the work terms and adiabaticity parameters contained in this preexponential factor are not known.

In contrast, our insulated electrode method affords the reorganization energy without requiring any knowledge of this preexponential term. In fact, we can independently determine the pre-exponential term from the rate/overpotential data. Due to the continuum of filled electronic states in the metal electrode, the electron transfer rate measured at electrode potentials more negative than the reorganization voltage does not decrease. Rather, electrons with energies below the Fermi level become more efficient at carrying out the electron transfer. At extremely negative potentials, the entire density of electronic states distribution is in resonance with filled states beneath the Fermi level of the metal electrode. Further polarization of the electrode to even more negative potentials does not result in an increase of the electron transfer rate. This maximal rate of electron transfer, k_{\max} , is not dependent on the extent of activation of the redox molecules but is determined by the probability of long-range electron tunneling from the Au surface to the cytochrome at closest approach to the monolayer-coated electrode. The k_{\max}

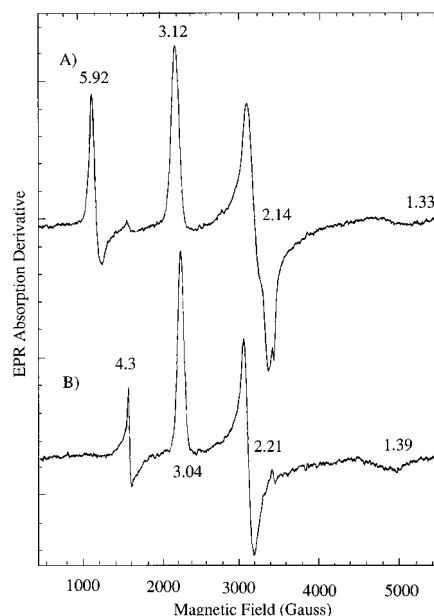


FIGURE 3: EPR spectra of (A) the A67V mutation of cytochrome b_5 and (B) wild-type rat cytochrome b_5 . Spectra were recorded at 12 K using 2 mW of microwave power at 9.51 GHz, using a modulation amplitude of 5 G at 100 kHz.

values measured for two different redox molecules at the same monolayer-coated electrode give a measure of the relative electronic coupling for the two redox molecules. As seen in Table 1, we also find that the electronic coupling between the wild type and A67V mutant is identical within the experimental error.

Spectroscopic Probes of the Electronic Structure of the Heme. (A) EPR Spectra. Significant differences between measured g -values for wild-type cytochrome b_5 and the A67V mutant were observed (see Figure 3). These shifts are indicative of significant changes in the d -orbital energy levels of the Fe in the heme system. We have interpreted these shifts using a crystal field approach using a t_{2g} electron hole formalism as previously described (Taylor, 1977). Inflections at g -values of 5.92 and 4.3 correspond to small contamination of free heme and adventitiously bound non-heme iron, respectively. The higher spin states of these contaminants significantly enhance their apparent relative intensity.

(B) NIR Spectra. Near infrared spectra of wild-type cytochrome b_5 and the A67V mutant (see Figure 4) are virtually identical, both containing maxima at 1660 nm. In other studies of cytochromes, bands in this region have been assigned to $a_{1u}(\pi)$, $a_{2u}(\pi) \rightarrow d_{yz}$, d_{xz} transitions (Schejter & Eaton, 1984). It is generally assumed that the highest occupied heme orbitals [e.g., $a_{1u}(\pi)$ and $a_{2u}(\pi)$ orbitals] are reasonably insensitive to changes in chemical environment, while the d_{yz} and d_{xz} orbitals are more sensitive to changes in the axial ligand orientation.

(C) NMR Spectra. Wide-spectral-width NMR spectra of the oxidized cytochromes were recorded over a range of temperatures to examine the effects of the mutation on the pattern of contact-shifted heme resonances. The temperature dependence of frequencies associated with the heme resonances of the A67V mutant protein is substantially altered relative to the wild-type protein (see Figure 5). Assignment of the contact shifted resonances was confirmed through an analysis of NOESY spectra as shown in Figure 6. The non-

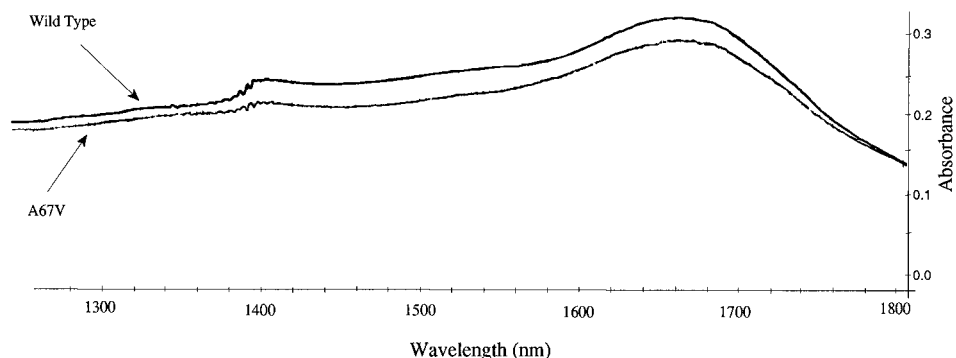


FIGURE 4: Near-IR spectra of wild-type cytochrome b_5 and the A67V mutations. Traces are labeled with the appropriate designation. Differences between the two curves reflect slight differences in concentration of the proteins.

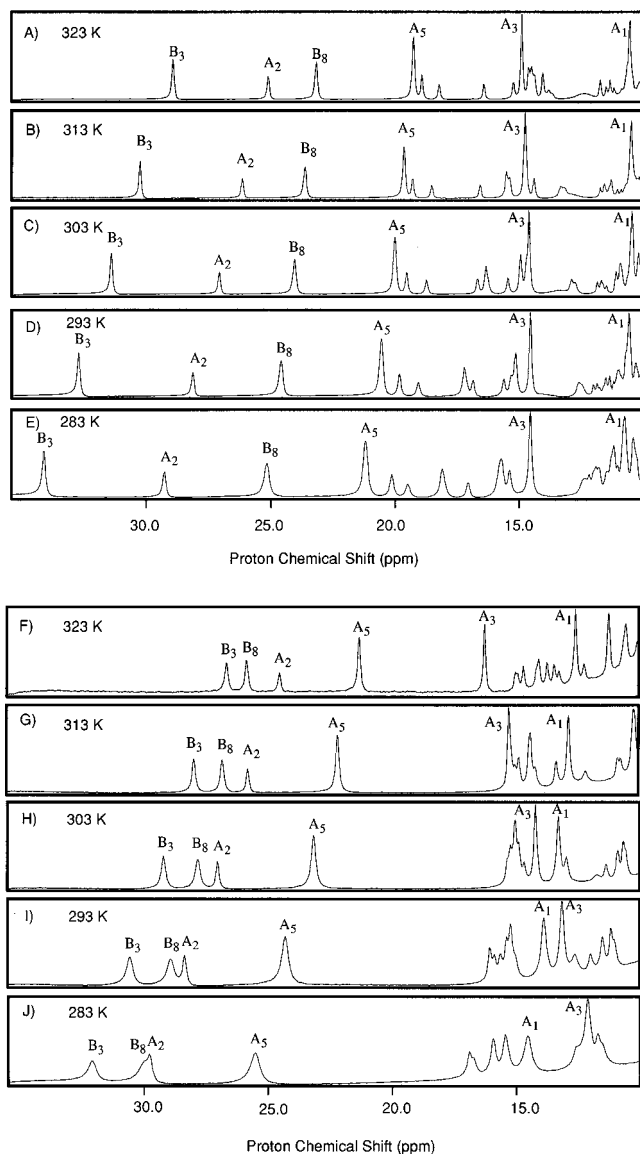


FIGURE 5: (A–E) NMR spectra of wild-type rat ferricytochrome b_5 recorded at the temperatures indicated and (F–J) NMR spectra of the A67V mutation recorded over the same range of temperatures. Spectra were recorded with a spectral width of 40 000 Hz at 600 MHz. Designations of contact-shifted resonances employ symbols used by Lee et al., 1993.

Curie temperature dependence of the methyl resonances of paramagnetic proteins was analyzed as recently described by Shokhirev and Walker (1996) by fitting the observed shift pattern to eq 1, which assumes a low-lying excited state that

is thermally accessible over the range of temperatures examined.

$$\delta_{n(\text{calc})}(T^*) = \frac{1}{T} \frac{W_1 F_{n1} + W_2 F_{n2} e^{-T^*/T}}{W_1 + W_2 e^{-T^*/T}} \quad (1)$$

$\delta_{n(\text{calc})}(T^*)$ are the calculated contact shifts at a given Boltzmann temperature difference, W_1 and W_2 are weighting factors determined by the spin state of the system (i.e., $W_1 = 2S_1 + 1$), T^* is the Boltzmann temperature difference (i.e., $T^* = (E_2 - E_1)/k_B$) and the constants F_{n1} and F_{n2} are determined by the best fit to the observed shifts at a given T^* value. Values for T^* for both A and B conformations of wild-type and mutant proteins were obtained by simultaneous nonlinear least squares fitting of resolved heme resonances for a range of T^* values spanning 0–4000 K. Least squares residuals for each value of T^* were generated by simultaneous simplex minimization of the n -methyl resonance terms in eq 2 measured at the m different temperatures. Well-defined minima were found for both A- and B-forms of both wild-type and mutant proteins.

$$\chi^2 = \sum_{m=1}^M \sum_{n=1}^N (\delta_{n(\text{calc})}(T_m) - \delta_{n(\text{obs})}(T_m))^2 \quad (2)$$

NMR spectra of wild-type and mutant proteins were recorded at 323, 313, 303, 293, and 283 K. The 1-methyl, 3-methyl, and 5-methyl resonances were used in fitting data of the A-form of wild-type and mutant cytochromes b_5 while the 3-methyl and 8-methyl resonances were used to fit the B-form of both proteins. Values for the energy difference between the ground state and the lowest lying excited state are summarized in Table 2. These energy level differences may be compared to values for the rhombic crystal field splitting parameter, V , obtained from an analysis of the EPR data described below, in that presumably the lowest lying thermally accessible excited state corresponds to the electronic configuration of the Fe(III) given by $(d_{xy})^2(d_{yz})^1(d_{xz})^1$. However, absolute energies are not obtained from the EPR analysis due to an uncertainty in the value of the spin-orbit coupling constant, ζ . If one assumes a value of the spin-orbit coupling constant in the range of 500 cm^{-1} , then agreement between the EPR and these temperature-dependent analyses is reasonable. Differences between the mutant and wild-type proteins are much more marked than differences between A- and B-forms. Note that values for all other measured parameters (with the exception of the susceptibility

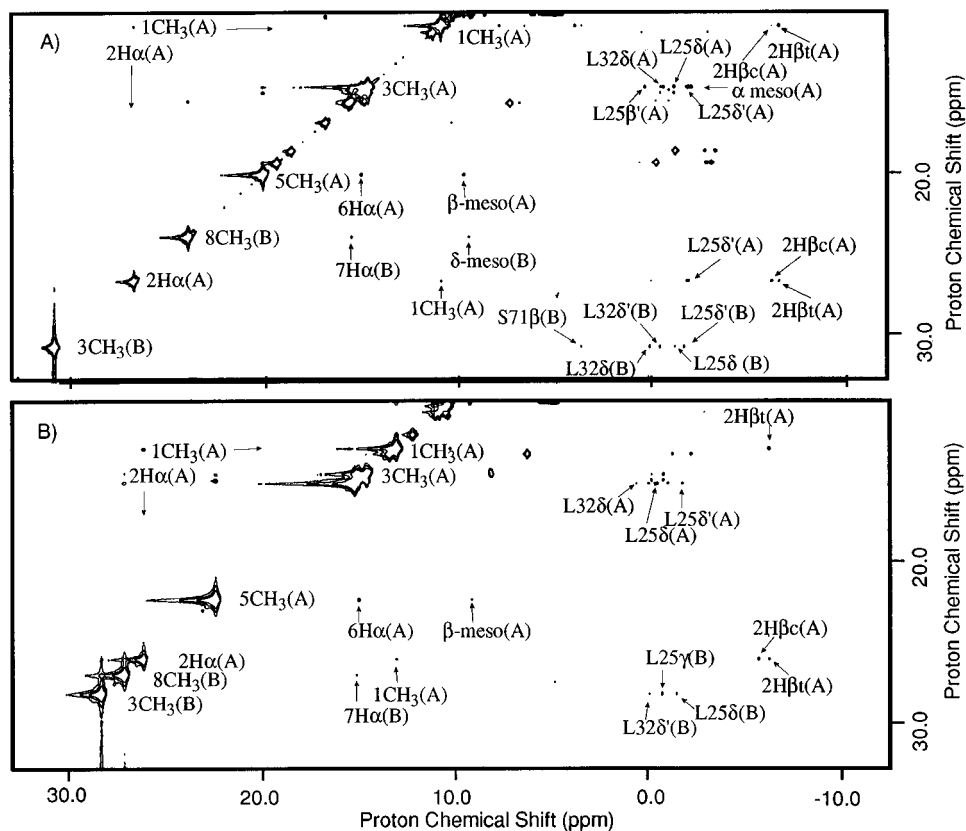


FIGURE 6: Regions of the NOESY spectra of (A) wild-type rat cytochrome *b*₅ and (B) the A67V mutation recorded at 313 K. The regions plotted illustrate NOESY connectivities which confirm assignments indicated in the panels in Figure 5. Designations for the heme resonances follow the nomenclature used by Lee et al. (1993). Full proton spectral widths are plotted along the *x*-axis while the *y*-axis is the same range that is plotted in Figure 5.

Table 2: Energy Level Differences between *d_{xz}* Orbitals Determined from the Temperature Dependence of the Contact-Shifted Resonances

	wild type		A67V	
	A-form	B-form	A-form	B-form
ΔE_{d_x} (cm ⁻¹) ^a	1480	1160	760	780

^a On the basis of the analysis of variance performed by Shokhirev and Walker (1995) we conservatively estimate the uncertainty in the ΔE_{d_x} values at 10% of the reported values assuming temperature variation is the dominant source of error.

tensors) reported in this paper reflect averages for the two different conformations which exist in slow exchange under the conditions of this study.

NOESY-related HSQC spectra of the reduced cytochromes *b*₅ were recorded with wide ¹⁵N spectral widths, in order to assign the resonances associated with imidazole nitrogen and proton frequencies. Figure 7 contains a region of the NOESY-related HSQC spectrum of wild-type cytochrome *b*₅ overlaid onto that of the A67V mutant which displays connectivities between the imidazole N δ correlation peaks and the main chain amides of H39 and H63. Note that the H39 resonances are virtually superimposed and that the changes in the amide protons of H63 are greater than the changes in proton frequencies of the N δ of the imidazole. The slight shifts which are observed in the nitrogen frequency of the N δ of H63 are in a direction which suggests a slight strengthening of the hydrogen bond to the carbonyl of F58.

Analysis of the Effect of the A67V Mutation on the d-Orbital Energy Levels. The effect of the A67V mutation on the *d*-orbital energy levels of the Fe of the heme system

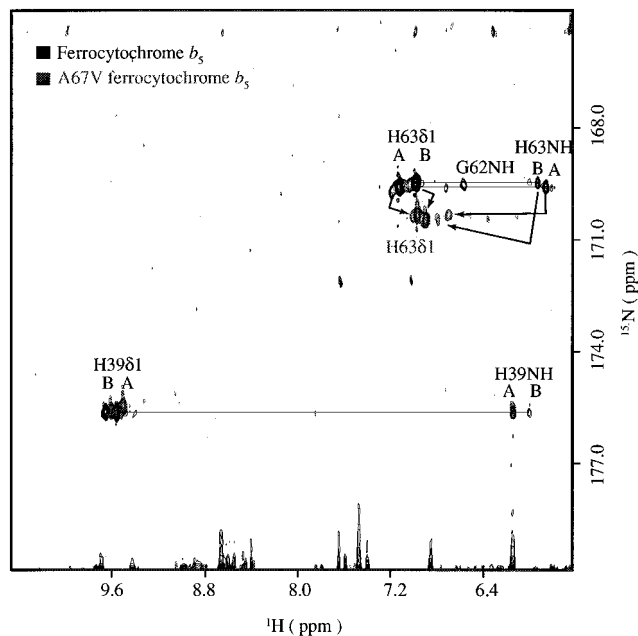


FIGURE 7: Overlay of 2D ¹H–¹⁵N HSQC–NOESY spectra of wild-type and mutant proteins indicating connectivities confirming the identities of the proton and ¹⁵N chemical shifts of N δ 1 atoms of both axial imidazoles. The ¹⁵N frequency of the N δ of the imidazole of H63 shows a small downfield shift in the mutant protein, indicating that the hydrogen bond is largely intact.

is schematically indicated in Figure 8. The dominant effect of the reorientation of the imidazole ring of histidine 63 appears to have been a destabilization of the *d_{xz}*-orbital energy level. We draw this conclusion on the basis of the analysis

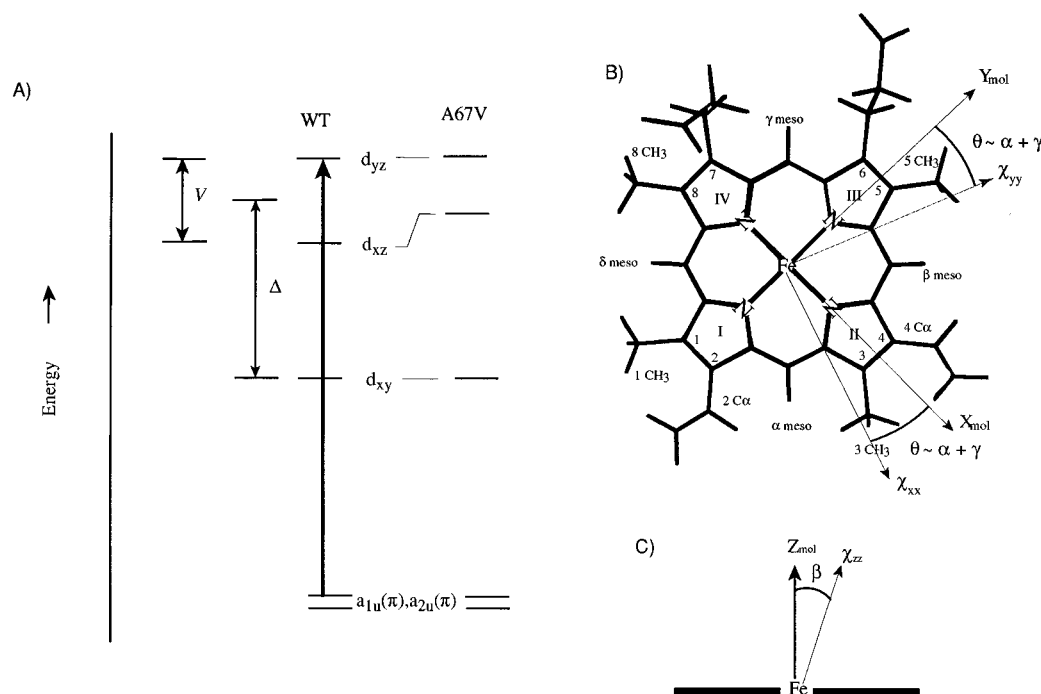


FIGURE 8: (A) Schematic d-orbital energy level diagram, illustrating differences between rhombic (V) and tetragonal (Δ) crystal field splittings in wild-type (WT) and mutant (A67V) cytochrome b_5 . The boldface vertical arrow indicates the origin and invariance of the near-IR transitions shown in Figure 5. (B) Definition of the in-plane rotation angle which defines the orientation of the electron hole and thus the orientation of χ_{xx} and χ_{yy} axes. The orientation of the axes shown reflects the in-plane rotation calculated for both wild type and the A67V mutation (see text for details). (C) Definition of out-of-plane rotation angle (β) which defines the orientation of χ_{zz} and excited-state orbital hole orientations which define the axes of magnetic anisotropy (see text for details). In this edge-on view of the heme, the heme plane is schematically indicated by the solid bars. The z -axis of the porphyrin system is defined as the heme normal with the origin at the iron.

of the EPR and NIR spectra of the wild-type and mutant proteins. Results from an analysis of the temperature dependence of the contact-shifted resonances described above are in agreement with the assertion of a compression of the rhombic field splitting.

The electronic configuration is assumed to be a low-spin Fe(III) $(d_{xy})^2(d_{yz}, d_{xz})^3$ configuration in a rhombically distorted axial ligand field. On the basis of g -values determined from the turning points in the low-temperature EPR spectra, it is possible to determine relative d-orbital energy levels. For a rhombically distorted axial crystal field two parameters are obtainable: the tetragonal field splitting parameter, Δ , and the rhombic field splitting parameter, V . The origin of magnetic anisotropy is spin-orbit coupling to excited electronic states. Mixing of excited-state orbital angular momentum results in a shift of the electron spin resonance from the free electron value. Admixture of excited states is reciprocally related to the energy level differences from the ground-state configuration. Thus, it is possible to relate the magnetic anisotropy to the magnitude of the d-orbital energy level differences.

Only relative energy level differences are obtainable due to uncertainty in the absolute value of the spin-orbit coupling constant. These solutions are not unique but depend upon certain assumptions regarding the signs of measured g -values and the choice of axis system. However, the solutions obtained provide clear insights into differences in the crystal field parameters between wild-type and mutant proteins, given the reasonably small perturbation induced by the mutation. Table 3 contains EPR parameters obtained from the low-temperature spectra and calculated values for Δ and V in units of ζ . Normalization values close to unity,

Table 3: EPR Parameters^a and Calculated Field Splitting Parameters^b

protein	g_x	g_y	g_z	Δ/ζ	V/ζ	V/Δ	$a^2 + b^2 + c^2$
wild type	1.39	2.21	3.04	3.17	1.60	0.50	1.0048
A67V	1.33	2.14	3.12	3.38	1.44	0.43	1.0026

^a EPR parameters derived from spectra recorded at 12 K. ^b Calculated values of field splitting parameters performed using the formalism developed by Taylor (see text for details).

which were not constrained in the approach of Taylor, add validity to the assumptions used in this analysis. Results from the analysis of the temperature dependence of the contact-shifted resonances presented above also provide some, at least, qualitative validation of the EPR analysis in that a compression of the rhombic field splitting parameter is also predicted. Relative to wild-type crystal field parameters, the mutant appears to have a larger tetragonal field splitting and a reduced rhombic splitting. In fact, the rhombicity of the A67V mutant is among the lowest of reported cytochromes (Walker et al., 1984). Because these calculations yield differences, it is also uncertain which energy levels are shifting on the basis of the EPR results alone.

Near-infrared bands associated with ligand to metal charge transfer transitions have been observed and assigned to $a_{1u}(\pi)$, $a_{2u}(\pi) \rightarrow d_{yz}$, d_{xz} transitions. These bands have been used to estimate absolute energy shifts of the lowest unoccupied d-orbitals in the Fe(III) state relative to the highest occupied molecular orbitals of the heme (Schejter & Eaton, 1984). Given the relative insensitivity of the heme molecular orbital energy levels to changes in the chemical environment of the heme, the variation in these bands has

been correlated with changes in the d_{yz} , d_{xz} -orbital energy levels. The stabilization or destabilization of the d_{xz} , d_{yz} energy levels has in turn been correlated with changes in reduction potential (Vincent et al., 1987). The apparent invariance of the band maxima in wild-type cytochrome *b*₅ and the A67V mutation indicates the d_{yz} -orbital has not changed in energy, as indicated in Figure 8A. In our analysis, the d_{yz} -orbital is assumed to be the highest energy d-orbital, containing the unpaired electron. Thus, the changes in d-orbital energy levels indicated by the analysis of the EPR data must be accomplished by shifts in d_{xy} - and d_{xz} -orbital energy levels. A destabilization of the d_{xz} orbital by about 0.2 ζ accounts for most of the observed differences between the A67V mutant and wild-type cytochrome *b*₅.

Analysis of the Reorientation of the d-Orbitals of the Iron. As described above, spin-orbit coupling is the origin of magnetic anisotropy. In addition, symmetry-allowed mixing of the d_{xz} - and d_{yz} -orbitals yields a rotation of the electron hole in the plane of the porphyrin ring which is dictated by the nature of the rhombic distortion (Shulman et al., 1971, LaMar & Walker, 1979). Symmetry-allowed mixing of $e(\pi)$ -orbitals has been used to describe contact shift patterns which result from this rotation. Mathematically, the resulting wavefunctions can be described by linear combinations of d-orbital wavefunctions and the porphyrin π orbitals of appropriate symmetry [e.g., $e(\pi)$]:

$$\psi_{yz} = a'\psi_{d_{yz}} + b'\psi_{e(\pi)} \quad (3)$$

$$\psi_{xz} = c'\psi_{d_{xz}} + d'\psi_{e(\pi)'}$$

where ψ_{yz} , ψ_{xz} are now molecular orbitals of the same symmetry as the d-orbitals from which they are derived and a' , b' , and c' are mixing coefficients.

These wavefunctions can then be combined to describe the in-plane rotation:

$$\psi'_{yz} = \psi_{yz} \cos \theta + \psi_{xz} \sin \theta \quad (4)$$

$$\psi'_{xz} = \psi_{xz} \cos \theta + \psi_{yz} \sin \theta$$

Thus, rotation of the electron hole in the porphyrin plane determines both the in-plane axes of magnetic anisotropy and the pattern of contact shifts observed by directing the unpaired spin density dominantly into a specific trans pair of pyrrole rings (e.g., rings I and III or II and IV). We suggest that the deviations of the magnetic axis system from the heme normal are analogously mediated through mixing of the strictly nonbonding $\psi_{d_{xy}}$ orbital into the molecular orbital containing the unpaired spin, ψ'_{yz} . Out-of-plane rotations described by the angle β in Figure 8C could be described identically to the effect of the in-plane rotations as shown below in eq 5.

Given the fact that magnetic anisotropy is determined by orientation-dependent spin-orbit coupling to excited-state electronic configurations, the orientation of the d-orbitals in these rhombically distorted systems is known and analytically described by the susceptibility tensor derived from the pseudocontact analysis presented in the accompanying paper. Thus, the orientation of the ψ_{yz} orbital expressed as a linear combination of d-orbital wavefunctions which are aligned with the molecular axis system of the heme can be represented in terms of the Euler angles as shown in eq 5.

Assuming β is small, the in-plane rotation, θ , is approximated by $\alpha + \gamma$. The direction of the tilt of the z -axis away from the heme is dictated by the angle, α .

$$\begin{aligned} \psi''_{yz} = & \psi_{yz}(\cos \alpha \cos \gamma - \sin \alpha \cos \beta \sin \gamma) - \\ & \psi_{xz}(\cos \alpha \cos \beta \sin \gamma + \sin \alpha \cos \gamma) - \psi_{d_{xy}}(\sin \beta \sin \gamma) \end{aligned} \quad (5)$$

It is important to note that eq 5 predicts that significant admixture of d_{xy} -orbital character into the orbital containing the unpaired spin density only occurs when significant γ rotations are present as is the case with the A67V mutant, but not the wild-type protein. For the A-forms of wild-type and the A67V mutant proteins the magnitudes of γ are 0° and 17°, respectively. This results in an admixture of only about 4.5% of the d_{xy} -orbital into the description of the ψ''_{yz} orbital as indicated by eq 5. It is expected that the effect of admixture of the $\psi_{d_{xy}}$ into the molecular orbital defining the z -axis tilt will have the additional effect of reducing the magnitude of contact shifts in general, in that the $\psi_{d_{xy}}$ is not of the appropriate symmetry to allow mixing with the porphyrin π -orbitals, and even in the reduced symmetry of the rhombically distorted system this mixing is likely to be small. Although linear combinations involving the d_{xy} -orbital have not been used to describe deviations from the heme normal in porphyrin systems to date, such mixing has been invoked in discussions of noncoincidences of g -tensors from the molecular axis systems in low-symmetry d1 systems (Scullane et al., 1979; Deijzers & deBoer, 1975).

In the cytochrome *b*₅ system, the effect of in-plane rotations (θ) on electrochemical properties (Walker et al., 1988) and contact and dipolar shifts have been examined in detail through the examination of species variants (Lee et al., 1993). Here, we have been able to examine the effect of differences in the direction of out-of-plane rotations (β) through site-directed mutagenesis of proteins as follows in the discussion section.

DISCUSSION

Effect of the Imidazole Ring Reorientation on Reduction Potential. A significant amount of experimental and theoretical work has been performed in an attempt to understand protein effectors of heme reduction potentials. Considerable bioinorganic modeling efforts have focused on the role of axial imidazole ligand plane orientation (Walker et al., 1984, 1986) and on the role of hydrogen bonding (Quinn et al., 1984; O'Brien et al., 1985). Here, we have focused on achieving axial ligand plane reorientation through the use of conservative heme binding pocket mutations. As indicated schematically in Figure 8A, contrary to previous theoretical descriptions of the effect of a simple rotation of the imidazole plane in the direction we have characterized, a stabilization of the highest occupied d-orbital due to decreased d-orbital interactions with the imidazole π -system was not observed. The effect of a simple rotation about the heme normal in the direction we observed would, in principle, have resulted in a decrease in the magnitude of the rhombic field splitting parameter with virtually no change in the tetragonal field splitting parameter (Walker et al., 1986). As indicated in the accompanying paper, a simple rotation of the axial imidazole was not achieved through conservative pocket mutations; a more complex gyration of the imidazole was

observed. However, it is clear that the destabilization of the d_{xz} -orbital is not the dominant origin of the shift in the reduction potential. On the basis of the apparent lack of change in the d_{yz} -orbital, it must be concluded that the observed change in reduction potential is largely due to stabilization of the highest occupied d-orbitals in the reduced state.

Although a more complex reorientation of the imidazole ring has occurred than a simple rotation, conceptually the reorientation of the ring can be broken down into components and their effects correlated with changes in the d-orbital energy levels. In the following discussion it is assumed that electrostatic repulsion between the d_{π} -orbitals and the imidazole π -system is the dominant energetic term contributing to changes in Fe d-orbital energy levels. A crystal field analysis of the effect of axial π -donor ligands such as imidazoles in porphyrin systems has been previously reported (Mims & Peisach, 1976). A simple crystal field approach would consider only electrostatic repulsion. More commonly, using a qualitative molecular orbital approach, "ligand back donation" is the mechanism invoked to describe the interaction which, because of its antibonding character, is also destabilizing in nature with respect to the d_{π} -orbitals. For illustration, two limiting cases might be considered: (1) For the case in which both axial π -donors have ligand planes aligned, the electrostatic repulsion with one of the two d_{π} -orbitals is maximized and the other minimized, yielding a maximum rhombic splitting. For example, using the definitions contained in Figure 8B, this would correspond to the situation where both imidazole planes were aligned along the pyrrole nitrogens of rings II and IV, resulting in a maximum destabilization of the d_{yz} -orbital. Although seemingly unfavorable, most model bis(imidazole) porphyrin complexes synthesized to date adopt a similar geometry with the imidazoles aligned along the N1–N3 porphyrin vector (Walker et al., 1986). (2) The opposite extreme is the case in which the planes of the two π -donors are orthogonal. In this case the destabilization of both d_{π} -orbitals is the same and the rhombic field splitting approaches zero.

The projection of the H63 imidazole plane onto the porphyrin plane can be taken as a measure of the degree of rotation of the imidazole about the heme normal (see Figure 8 of the accompanying paper). On the basis of the solution structure calculations of the changes in the mutant determined in the accompanying paper, the projection for the H63 imidazole of the mutant is rotated away from the wild-type orientation toward a closer alignment with the axis defined by the nitrogens of pyrrole rings I and III. In fact, the mean magnitude of this rotation, 17° , is equal to the degree of rotation of the z -component of the susceptibility tensor induced by mutation, described below. This rotation component of the reorientation further separates the projections of H63 and H39 imidazole planes in the mutant (approaching case 2 in the examples above), resulting in a predicted compression of the rhombic field splitting parameter as is observed. In addition, the H63 ring has apparently been slightly tilted toward the porphyrin plane in the direction of pyrrole ring II in the mutant. This structural change would result in greater electronic repulsion of both d_{π} -orbitals, or a predicted increase in the tetragonal field splitting parameter as is also observed. More conventional wisdom would indicate the distortion resulted in a stronger ligand field due to the altered imidazole geometry which increased σ -bonding

character and hence the ligand field strength (Blumberg & Peisach, 1971). However, the nature of the reorientation would seem to be far from optimal for imidazole nitrogen donation. As indicated in Figure 8A, the net effect of a compression in V and an expansion in Δ results in no net change in the energy of the d_{yz} -orbital. Thus, surprisingly the stabilization of the d-orbitals in the reduced state must play a more important role in dictating reduction potentials than has previously been thought.

Role of Hydrogen Bonding. On the basis of the relatively small shifts observed in both proton and ^{15}N resonances of the imidazole ring in the reduced state, it would appear that, contrary to initial expectations, the hydrogen bond between the H63 N δ proton and the F58 carbonyl appears to have remained largely intact. Given the direction of the small changes in the chemical shifts observed in the A67V mutation relative to the wild-type protein, a slight strengthening of the hydrogen bond might be assumed. Note that the changes are in the opposite direction to shifts in characterized systems where the hydrogen bond has been broken (Smith et al., 1989). Presumably, a continuum of inductive effects spanning optimum hydrogen bond strength to free imidazolate would be evident in the ^{15}N resonance frequency observed. Note that the direction of the shift in the reduction potential is in the direction expected based on previous bioinorganic modeling studies (Quinn et al., 1984; O'Brien et al., 1985). On the basis of these studies, it is estimated that the maximum effect of hydrogen bonding on the reduction potential is roughly 60 mV. Assuming the effect is linear, this would scale to a 5 mV shift in the reduction potential in the direction observed, based on the observed changes in ^{15}N chemical shift. Therefore, it is concluded that the modulation of the hydrogen bond strength was not the major factor mediating the observed changes in the reduction potential.

Reorientation of the Susceptibility Tensor, Altered Contact Coupling, and Inferences as to the Mechanism of Electronic Coupling. As described in greater detail above, in the absence of anisotropic axial ligand interactions, assuming the porphyrin system is of pseudo- D_{4h} symmetry, an infinitely degenerate set of solutions exists for the wavefunctions describing the degenerate pair of largely nonbonding d-orbitals of π -symmetry (e.g. d_{xz} , d_{yz} using real basis functions). The small degree of mixing between these wavefunctions and the porphyrin π -system results in the contact shifts observed in the methyl, vinyl and propionate resonances of the protoporphyrin IX ring system. In the presence of a rhombic field, unique solutions for the two d_{π} -orbitals exist and the extent of electron delocalization is a sensitive function of the exact solution which dictates the extent of mixing. The solutions obtained also dictate the orientation of the axis system describing the magnetic anisotropy due to spin-orbit coupling with low lying excited-state configurations. Thus, both the dipolar coupling tensor, or pseudo-contact tensor orientation, and the nature of the contact shifts observed are dictated by the nature of the rhombic distortion.

Several physical mechanisms have been invoked to describe the origin of the noncoincidence of magnetic and molecular axis systems responsible for these two effects (e.g., the orientation of the susceptibility tensor and the pattern of contact shifted resonances). To date, proposed mechanisms include Jahn–Teller effects (Schulman et al., 1971), crystal field effects due the planar imidazole ligands (Mims &

Piesach, 1976), and thermal mixing of low-lying excited states (Shokhirev & Walker, 1995). On the basis of our analysis of the temperature dependence of the contact-shifted resonances for wild-type and mutant proteins, it would appear that thermal mixing of an excited-state configuration involving principally d_{xz} -orbital character into the ground state is not likely to result in significant in-plane rotations due to the fact that the energy level differences determined are several times $k_B T$ even in the most favorable case, that of the A67V mutant. This result is further supported by the fact that the magnitude of the in-plane rotation determined from the pseudocontact calculations is identical for mutant and wild-type proteins despite significant differences in Δd_{τ} . Clearly, deviations of the magnetic axis systems from the heme normal are even less likely to be due to thermal mixing of the d_{xy} -orbital due to even larger energy level differences. Reasonable agreement between magnetic anisotropy determined from low-temperature single-crystal EPR studies (Palmer, 1983) and room temperature pseudocontact analyses for a number of heme proteins also indicates that thermal mixing is not a significant mechanism leading to noncoincidence of magnetic and molecular axes.

Further support for the hypothesis that the dominant term contributing to the reorientation of the susceptibility tensor and hence the d-orbitals is due to the ligand field comes from a number of recent detailed susceptibility tensor analyses. In the case of cytochrome *c* (Feng et al., 1990; Gochin & Roder, 1995), cyanometmyoglobin (Emerson & LaMar, 1990), and site-directed mutants of cyanometmyoglobin (Rajaratnam et al., 1993), the *z*-axis of the susceptibility tensor is directed along the axis of the dominant axial ligand (Fe–S in the case of cytochrome *c* and Fe–C in the case of cyanometmyoglobin), i.e., the shortest bond length. If the *z*-axis is directed along this bond, then based on a crystal field approach the repulsion between the ligand field and the reoriented t_{2g} orbital set is minimized. The case of cytochrome *b*₅ is more complex in that clearly both imidazole nitrogens must play some role; however, our result suggests that the H63 imidazole nitrogen plays the dominant role in dictating the orientation of the *z*-axis tilt.

Recently, an analysis of contact and dipolar shift patterns observed in a set of species variants of cytochrome *b*₅ was performed which indicated that both the magnitude of contact shifts and the orientation of in-plane components of the dipolar coupling tensor are dictated by the orientation of the porphyrin ring system relative to the H39 imidazole ring which is rigidly fixed by hydrogen bonding to the main chain carbonyl of G42. Reorientation of the porphyrin was mediated in these natural species variants due to differing steric bulk of hydrophobic residues in contact with the heme.

In this report, we have found that reorientation of the H63 imidazole does not affect the in-plane dipolar coupling tensor components as suggested by Lee et al. (1993), but the direction of the *z*-component of magnetization has been reoriented and in addition the contact shift pattern has shifted in a manner deviating from the proposed model, indicating that both the orientation of the in-plane components and the orientation of the *z*-component strongly influence the mixing of the d_{τ} -orbitals with the porphyrin π -system. We have suggested that mixing of the d_{xy} orbital with the d_{τ} -orbitals is responsible for the *z*-axis tilt, in a manner totally analogous to in-plane rotations described by Shulman et al. (1971), and that the degree of mixing is analytically described by the

Euler angles derived from the pseudocontact shift analysis. Because mixing of the d_{xy} -orbital with the π -orbitals of the heme is symmetry forbidden in axial symmetry (e.g., D_{4h}) and presumably weak even with a rhombic distortion, the effect of this admixture would be a reduction in contact coupling. Surprisingly, this was not observed. The pattern of contact shifts, although significantly altered, is not generally reduced in magnitude. However, it is conceivable that mixing of the d_{xy} -orbital into the heme molecular orbitals could occur if a symmetric puckering of the heme ring occurred (Safo et al., 1994). The result of this mixing would not be a net reduction in contact coupling but an altered pattern as was observed. Surprisingly, *ab initio* calculations of the effect of this symmetric, so-called S_4 ruffling of the heme would result in relatively small changes in heme molecular orbital energy levels (Perrin, 1973) as is consistent with the observations of very small perturbations in both UV–visible and NIR bands.

A similar reorientation of the electron hole orientation due to a twist of the porphyrin plane caused by steric interactions of axial pyridines with bulky meso substituents has apparently resulted in a $(d_{yz}, d_{xz})^4(d_{xy})^1$ ground-state configuration due to a S_4 distortion (Safo et al., 1994). This might be considered a limiting case of the *z*-axis tilts we have observed in cytochrome *b*₅. At present, the NMR analysis of the structural changes in cytochrome *b*₅ is not sufficiently accurate to conclude that this type of distortion of the porphyrin is responsible for the apparent mixing of d_{xy} -orbital character into the description of the electron hole. We have suggested that the slight tilt of the imidazole plane away from the heme normal is the origin of both the increased tetragonal field splitting and the tilt of the *z*-axis of the magnetic anisotropy.

We also suggest that the pattern of delocalization of the d_{τ} -electron spin density into the porphyrin π -system and the distance of the heme edge from the electrode may be correlated with the strength of electronic coupling of the cytochrome with the electrode. The extent of delocalization of the dI hole into the π -system must mediate the ease with which the electrode is able to transfer electrons into the π -system of the porphyrin and thereby into the vacant d-orbital of the iron. Recent electrochemical studies that we have performed on cytochrome *c* (Terrettaz et al., 1996) indicate that the reorganizational energy of cytochrome *c* is slightly higher than that of cytochrome *b*₅ and yet the electronic coupling, indicated by the heterogeneous rate of electron transfer, is greater. This is surprising given the fact that the crystal structures indicate that the solvent-exposed heme surface is greater for the case of cytochrome *b*₅ (i.e., the solvent-accessible surface calculated for cytochrome *b*₅ is roughly 3.9% of the total surface while that of cytochrome *c* is about 0.9%). However, in the case of cytochrome *c* the side of the heme exposed is on the side of the β -meso while that of cytochrome *b*₅ is that of the γ -meso edge. Thus, the propionates on the exposed edge of cytochrome *b*₅ must prevent a close approach of the heme to the electrode surface.

Given the differences in the pattern of contact coupling observed between mutant and wild-type cytochrome *b*₅, one might have predicted an alteration in the strength of electronic coupling to the electrode. The fact that the electronic coupling observed in mutant and wild-type proteins was indistinguishable suggests that there is an ensemble of coupling pathways in the mutant and wild-type proteins, the

weighting of the sum of individual pathways differing but the net coupling remaining invariant. This suggestion is more consistent with medium models which do not depend on the nature of the protein structure between the redox-active metal center and the electrode.

REFERENCES

- Basu, P., Shokhirev, N. V., Enemark, J. H., & Walker, F. A. (1995) *J. Am. Chem. Soc.* **117**, 9042–9055.
- Becka, A. M., & Miller, C. J. (1992) *J. Phys. Chem.* **96**, 2657–2668.
- Blumberg, W. E., & Peisach, J. (1971) *Adv. Chem. Ser.* **100**, 271–291.
- Bushnell, G. W., Louie, G. W., & Brayer, G. D. (1990) *J. Mol. Biol.* **214**, 585–595.
- Deijzers, C. D., & deBoer, E. (1975) *Mol. Phys.* **29**, 1007–1020.
- Dixon, D. W., Hong, X., Woehler, S. E., Mauk, A. G., & Sishta, B. P. (1990) *J. Am. Chem. Soc.* **112**, 1082–1088.
- Feng, Y., Roder, H., & Englander, S. W. (1990) *Biochemistry* **29**, 3493–3504.
- Friesner, R. A. (1994) *Structure* **2**, 339–342.
- Funk, W. D., Lo, T. P., Mauk, M. R., Brayer, G. D., MacGillivray, R. T. A., & Mauk, A. G. (1990) *Biochemistry* **29**, 5500–5508.
- Gochin, M., & Roder, H. (1995) *Protein Sci.* **4**, 296–305.
- Goodin, D. B., & McRee, D. E. (1993) *Biochemistry* **32**, 3313–3324.
- Guiles, R. D., Basus, V. J., Sarma, S., Malpure, S., Fox, K. M., Kuntz, I. D., & Waskell, L. (1993) *Biochemistry* **32**, 8329–8340.
- LaMar, G. N., & Walker, F. A. (1979) in *The Porphyrins* (Dolphin, D., Ed.) Vol. IV, pp 86–88, Academic Press, New York.
- LaMar, G. N., & deRopp, J. S. (1993) in *Biological Magnetic Resonance: NMR of Paramagnetic Molecules* (Berliner, L. J., & Rueben, J., Eds.) Vol. 12, pp 57–73, Plenum Press, New York.
- Langen, R., Brayer, G. D., Berghuis, A. M., McLendon, G., Sherman, G., & Warshel, A. (1992) *J. Mol. Biol.* **224**, 589–600.
- Langridge, R., Ferrin, T. E., Kuntz, I. D., & Connolly, M. L. (1981) *Science* **211**, 661–666.
- Lee, K.-B., LaMar, G. N., Mansfield, K. E., Smith, K. M., Pochapsky, T. C., & Sligar, S. G. (1993) *Biochim. Biophys. Acta* **1202**, 189–199.
- Livingston, D. J., McLachlan, S. J., LaMar, G. N., & Brown, W. D. (1985) *J. Biol. Chem.* **260**, 15699–15707.
- Mathews, F. S. (1985) *Prog. Biophys. Mol. Biol.* **45**, 1–56.
- Mathews, F. S., Czerwinski, E. W., & Argos, P. (1979) in *The Porphyrins* (Dolphin, D., Ed.) Vol. VIII, pp 107–147, Academic Press, New York.
- McLachlan, S. J., LaMar, G. N., & Lee, K. B. (1988) *Biochim. Biophys. Acta* **957**, 430–445.
- Mims, W. B., & Peisach, J. J. (1976) *J. Chem. Phys.* **64**, 1074–1091.
- O'Brien, P., Sweigart, D. A. (1985) *Inorg. Chem.* **24**, 1405–1409.
- Palmer, G. (1979) in *The Porphyrins* (Dolphin, D., Ed.) Vol. IV, pp 313–353, Academic Press, New York.
- Perrin, M. H. (1973) *J. Chem. Phys.* **59**, 2090–2104.
- Poulos, T. L., & Mauk, A. G. (1983) *J. Biol. Chem.* **258**, 7369–7373.
- Press, W. H., Teukolosky, S. A., Vetterling, W. T., & Flannery, B. P. (1992) *Numerical Recipes in FORTRAN, the Art of Scientific Computing*, pp 387–448, Cambridge University Press, Cambridge.
- Quinn, R., Mercer-Smith, J., Burstym, J. N., & Valentine, J. S. (1984) *J. Am. Chem. Soc.* **106**, 4136–4144.
- Rajaram, K., Qin, J., LaMar, G. N., Chiu, M. I., & Sligar, S. G. (1993) *Biochemistry* **32**, 5670–5680.
- Reid, L. S., Gray, H. B., Dalvit, C., Wright, P. E., & Saltman, P. (1987) *Biochemistry* **26**, 7102–7107.
- Rodgers, K. K., & Sligar, S. G. (1991) *J. Mol. Biol.* **221**, 1453–1460.
- Safo, M. K., Gupta, G. P., Walker, F. A., & Scheidt, W. R. (1991) *J. Am. Chem. Soc.* **113**, 5497–5500.
- Safo, M. K., Walker, F. A., Raitsimring, A. M., Walters, W. P., Dolata, D. P., Debrunner, P. G., & Scheidt, W. R. (1994) *J. Am. Chem. Soc.* **116**, 7760–7770.
- Salemme, F. R. (1976) *J. Mol. Biol.* **102**, 563–568.
- Sarma, S., Dangi, B., Yan, C.-H., DiGate, R. J., Banville, D., & Guiles, R. D. (1997) *Biochemistry* **36**, 5645–5657.
- Schejter, A., & Eaton, W. A. (1984) *Biochemistry* **23**, 1081–1084.
- Schulman, R. G., Glarum, S. H., & Karplus, M. (1971) *J. Mol. Biol.* **57**, 93–115.
- Scullane, M. I., Taylor, R. D., Minelli, M., Spence, J. T., Yamanouchi, K., Enemark, J. H., & Chasteen, N. D. (1979) *Inorg. Chem.* **18**, 3213–3219.
- Shokhirev, N. V., & Walker, F. A. (1995) *J. Phys. Chem.* **99**, 17795–17804.
- Siddarth, P., & Marcus, R. A. (1993) *J. Phys. Chem.* **97**, 2400–2405.
- Smith, S. O., Farr-Jones, S., Griffin, R. G., & Bachovchin, W. W. (1989) *Science* **244**, 961–964.
- Stayton, P. S., Poulos, T. L., & Sligar, S. G. (1981) *Biochemistry* **28**, 8201–8205.
- Taylor, C. P. S. (1977) *Biochim. Biophys. Acta* **491**, 137–149.
- Terrettaz, S., Becka, A. M., Traub, M. J., Fetting, J. C., & Miller, C. J. (1995) *J. Phys. Chem.* **99**, 11216–11224.
- Terrettaz, S., Cheng, J., Miller, C. J., & Guiles, R. D. (1996) *J. Am. Chem. Soc.* **118**, 7857–7858.
- Vincent, J. S., Kon, H., & Levine, I. W. (1987) *Biochemistry* **26**, 2313–2314.
- Walker, F. A., Huynh, B. H., Scheidt, W. R., & Osvath, S. R. (1986) *J. Am. Chem. Soc.* **108**, 5288–5297.
- Walker, F. A., Emrick, D., Rivera, J. E., Hanquet, B. J., & Buttlare, D. H. (1988) *J. Am. Chem. Soc.* **110**, 6234–6240.
- Wendoloski, J. J., Matthew, J. B., Weber, P. C., & Salemme, F. R. (1987) *Science* **238**, 794–797.
- Zhou, H.-X. (1994) *J. Am. Chem. Soc.* **116**, 10362–10375.

BI961859P